General Disclaimer

One or more of the Following Statements may affect this Document

- This document has been reproduced from the best copy furnished by the organizational source. It is being released in the interest of making available as much information as possible.

- This document may contain data, which exceeds the sheet parameters. It was furnished in this condition by the organizational source and is the best copy available.

- This document may contain tone-on-tone or color graphs, charts and/or pictures, which have been reproduced in black and white.

- This document is paginated as submitted by the original source.

- Portions of this document are not fully legible due to the historical nature of some of the material. However, it is the best reproduction available from the original submission.

Produced by the NASA Center for Aerospace Information (CASI)

DESERT RESEARCH INSTITUTE
UNIVERSITY OF NEVADA SYSTEM

F I N A L   R E P O R T

"MODIFICATION OF THE CONTINUOUS
FLOW DIFFUSION CHAMBER
FOR USE IN ZERO-GRAVITY"

AUTHORED BY

GARY KEYSER

CONTRACT TITLE: STUDY OF ZERO-GRAVITY ATMOSPHERIC
CLOUD PHYSICS LAB CHAMBER DEVELOPMENT
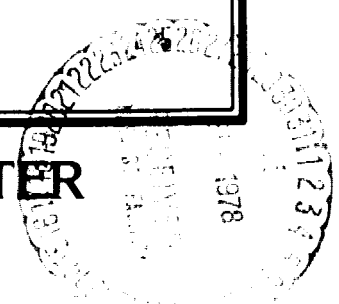
CONTRACT NO: NAS8-31470

CONTROL NO: NONE   COPY NO: NONE

PERIOD COVERED: MAY 13, 1975 THROUGH JUNE 30, 1978

DESERT RESEARCH INSTITUTE
ATMOSPHERIC SCIENCES CENTER
SAGE BUILDING, STEAD CAMPUS
RENO, NV 89506

AUGUST 1978

ATMOSPHERIC SCIENCES CENTER

TABLE OF CONTENTS

1.0 INTRODUCTION

The following report is a general summary of the philosophy of design and the performance characteristics of the Continuous Flow Diffusion Chamber (CFD) developed for the National Aeronautics and Space Administration (NASA) for use in ground-based simulation of some of the experiments planned for ACPL I during the first flight of Spacelab. Some of the problems encountered with design concepts and hardware are also discussed, along with recommendations concerning component testing and possible further development of this type of cloud-forming instrument.

The new CFD is based upon the cloud chambers developed by Hudson and Squires reported in 1973 and 1976, and on a theoretical study done under this contract.

The new instrument provides the capability of controlling a super-saturation spectrum of an aerosol as required in the ACPL Cloud-Forming and other experiments to an accuracy of about 1%. The instrument is auto-mated to cycle through several supersaturations in a very short period of time. These accuracy and speed capabilities are not found with older labora-tory equipment, and are equivalent to the capabilities that are specified for the flight hardware of the ACPL. The equipment is shown in Figures 1 and 2. The power requirements for this equipment are shown in Table I. Fabrication drawings will be made available to the NASA upon request.

2.0 PRINCIPLE OF OPERATION

The instrument incorporates two wet thermal surfaces maintained at a well known and stable temperature difference. The linear temperature grad-ient between the wet surfaces establishes a supersaturated vapor field bet-ween the plates, through which particle-free air is drawn at a flow rate of from 15 to about 75 cm^3/sec. About 8 cm downstream of the carrier flow entrance, after approximate temperature equiliberation has occurred, an aerosol is injected into the center of the chamber in the form of a thin lamina. Dimensions of the lamina are approximately 0.05 x 8.0 cm. Since the thermal plates are 29 cm wide, any perturbing effects caused by the side walls of the chamber are minimized, and the aerosol sample is exposed to a well-defined supersaturation. As the sample lamina flows between the
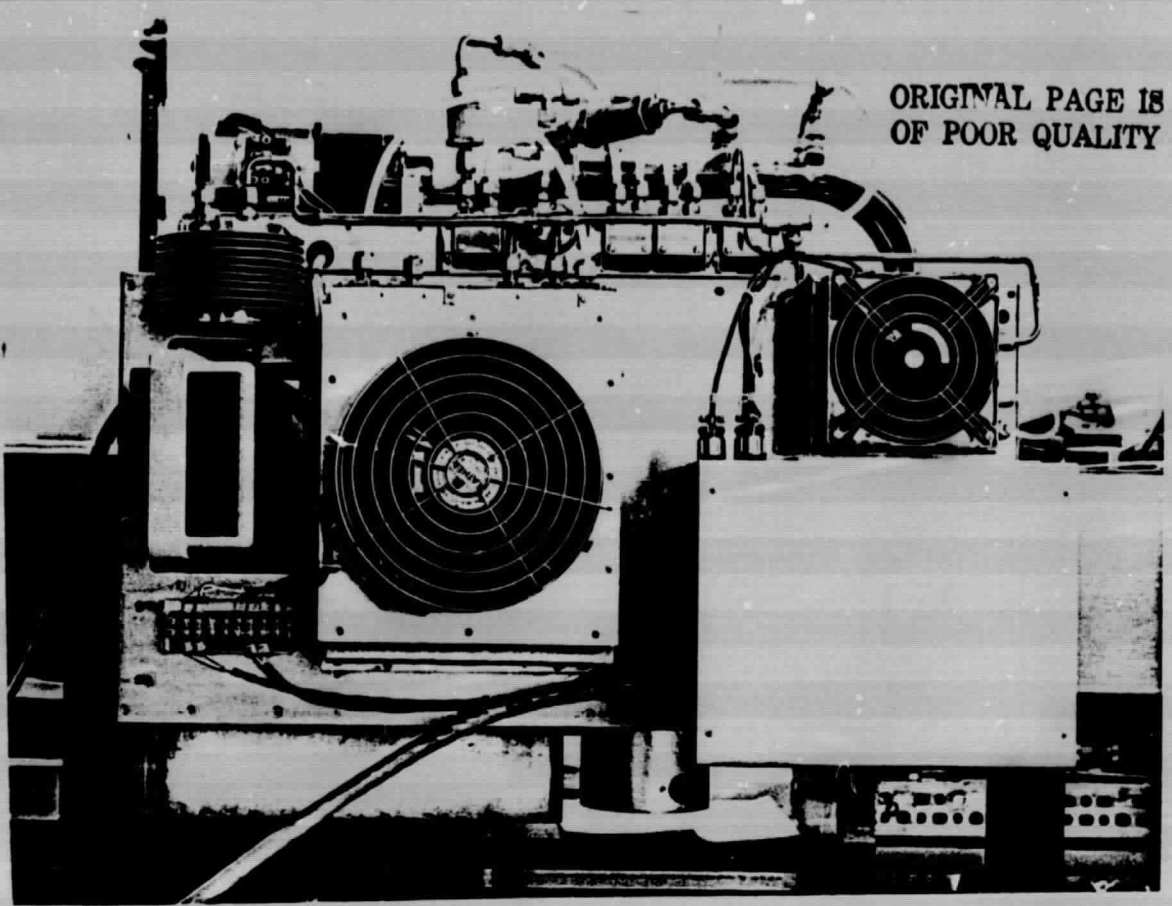
Figure 1. Side view of continuous flow
diffusion chamber.

Figure 2. Front view of CFD control
rack and Teletype. Equip-
ment in the rack from the
top is:
① Air flow control panel
② Royco 225 mainframe

③ Computer and power supply

④ 28 VDC supply
⑤ TEM waste heat radiators

TABLE I. CFD POWER REQUIREMENTS

UNIT	SOURCE	POWER (watts)
Computer and Power Supplies	115 VAC, 60 Hz	530
Cooling Fans (4)		80
Circulation Pumps (8)		90
	Sub Total	700
Royco 225	115 VAC, 60 Hz	225
Teletype		575
	Sub Total	800

chamber walls, micron-sized droplets are formed on the aerosol particles. The size distribution of these cloud droplets is determined photo-electrically with the use of an Optical Particle Counter (OPC) at the exit of the chamber. Schematically, the apparatus is shown in Figure 3; the principle is discussed in more detail by Hudson and Squires (1973 and 1976).

3.0 THERMAL CONTROL OF THE INSTRUMENT

The thermal plates of the CFD are controlled to cycle through several temperature steps around a fixed mean temperature for each experiment, allowing a spectra of supersaturations to be examined. A hypothetical experiment is shown in Figure 4. Each supersaturation (temperature difference) can be maintained as long as desired to allow adequate time for counting; the subsequent supersaturation is established and stable after a period of from 10 to 30 seconds. Thus, the experiment can proceed at a rapid rate, allowing some flexibility when scheduling concurrent experiments.

Each thermal plate is accurately controlled in temperature such that the temperature difference between the two plates is stable and known to within about ±0.01°C for each supersaturation. Both the warm and the cold plate can be controlled independently in a range from about 2°C to ambient. The maximum temperature difference measurable between the plates is 10°C.

Figure 5 is a schematic of the hydraulic circuit for the warm thermal plate. A centrifugal pump circulates water through the thermal plate and a housing containing four electrically resistive emersion heaters at a rate of about 60 cm^3/sec. (1.0 gal/min.) The water is also circulated over a small glass bead thermistor just downstream of the pump; this method of temperature measurement provides an accurate esti-mate of the average temperature because of the thorough mixing present at the pump exit. The thermal plate consists of a covered channeled metal surface with large distribution manifolds at both ends. The large mani-folds assure that flow through each of the 18 water channels is uniform. Placing the exit and entrance ports on the same side of the thermal

4

Figure 3. Physical schematic of chamber.
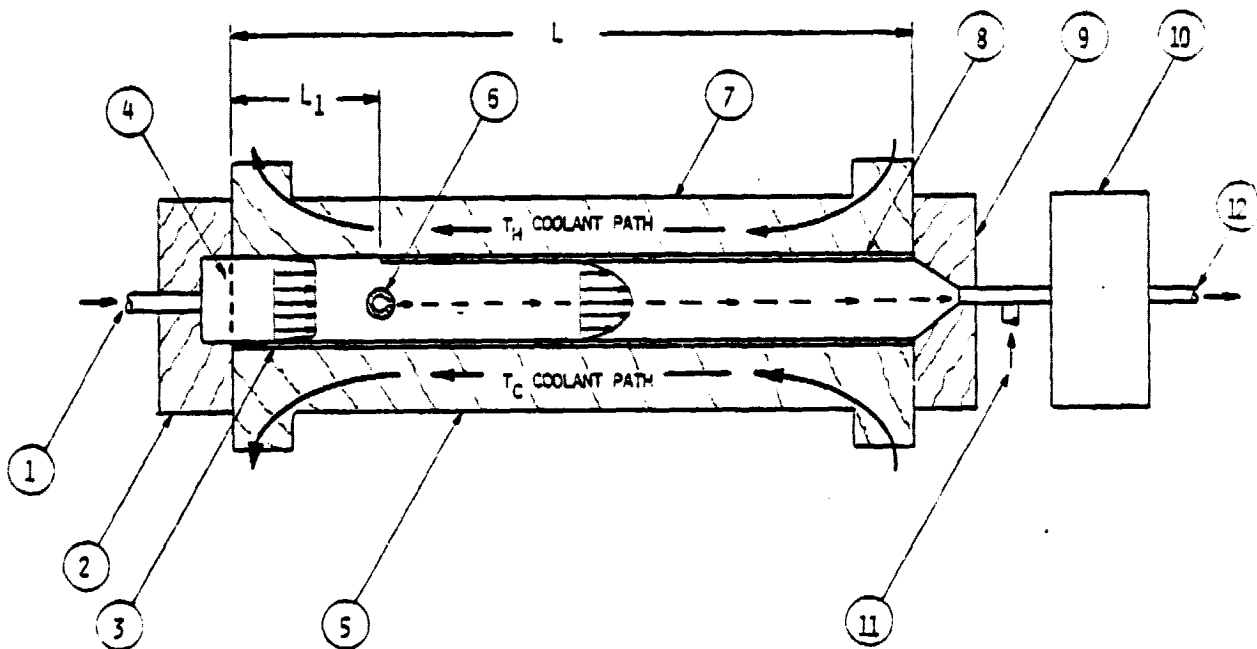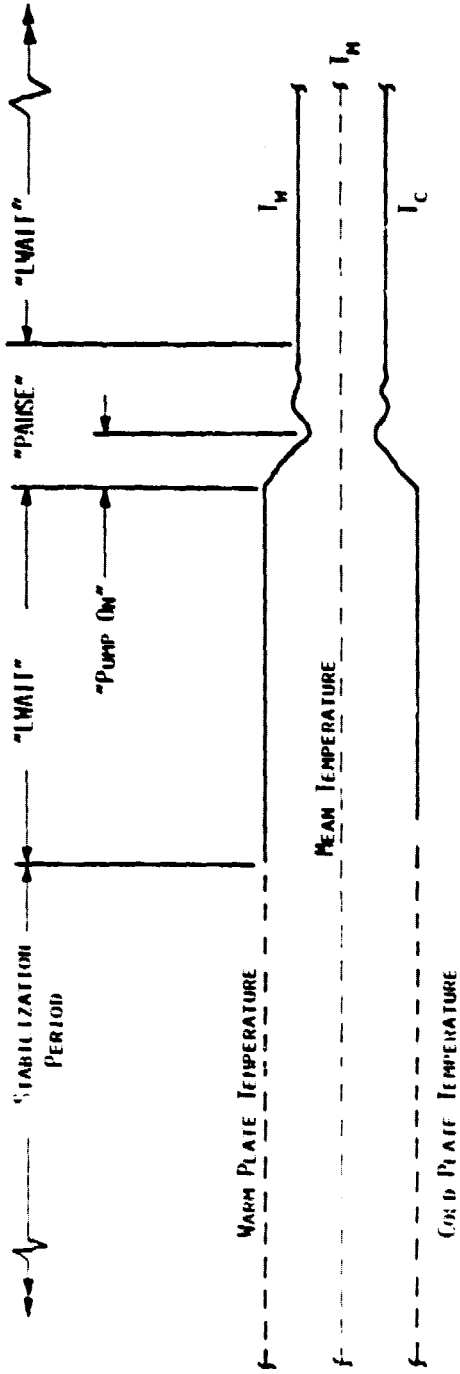
Legend:

1. Carrier flow entrance
2. Entrance manifold
3. Cold plate wicking surface
4. Diffuser screen
5. Cold thermal plate
6. Sample injection tube
7. Warm thermal plate
8. Warm plate wicking surface
9. Exhaust manifold
10. Optical particle counter
11. Sheath flow entrance
12. OPC exhaust

Dimensions:

L = 44.45 cm
L_1 = 10 cm
Width = 29 cm
Plate spacing = 1.6 cm

EVENT SEQUENCE:

1. STABILIZATION: About 15-20 minutes is required to allow the CFD to become equilibrated at the initial temperature settings.

2. "LWAIT" PERIOD: The experiment is initiated by a manual command at the start of "LWAIT". This period is long enough to allow sufficient time for counting particles in the CFD.

3. "PAUSE": Counting stops at the end of the "LWAIT" period. "PAUSE" allows time for the system to stabilize at new temperature settings. This has been a period of about 30 seconds in preliminary experiments. The end of "PAUSE" initiates another "LWAIT" period at a new supersaturation. The instrument continues to sequence until ΔT reaches a predetermined minimum.

Figure 4. Temperature control of the thermal plates of the CFD is programmed to follow the sequence shown above.
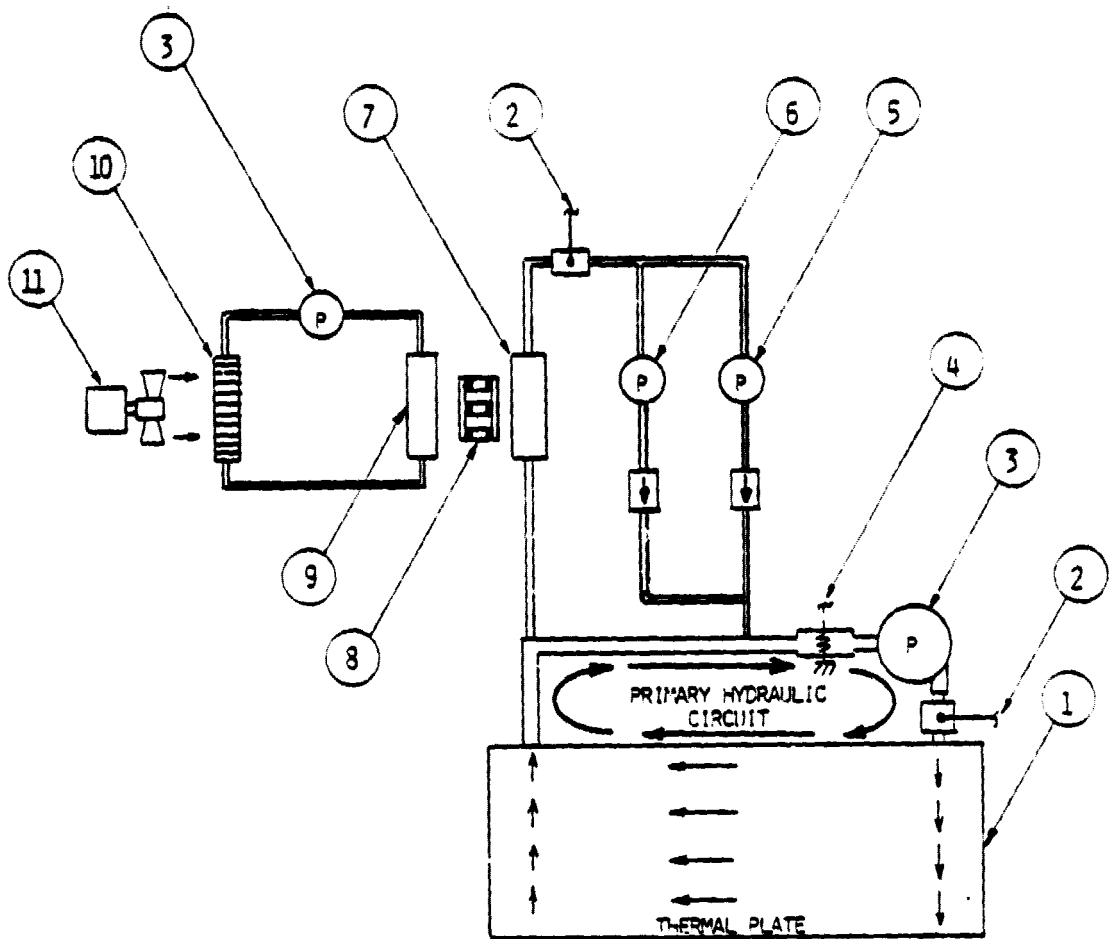
6

Figure 5. Schematic representation of hydraulic circuit

Legend:

1. Thermal plate
2. Thermistor
3. Centrifugal pump
4. Servo heater
5. Trickle pump
6. Surge pump
7. Cold source heat exchanger
8. Thermoelectric module
9. Water jacket
10. Waste heat radiator
11. Fan

plate assures kinematic mixing of the water in the Primary Circuit. The time required for a parcel of water to flow completely around the Primary Circuit is one to two seconds.

Temperature control is provided by a secondary hydraulic circuit consisting of a thermoelectric module (TEM) powered "cold source" heat exchanger and a small gear pump. Since this is a closed hydraulic system, operation of the gear pump (trickle pump) displaces cold water into the Primary Circuit and returns warmer water to the cold source heat exchanger. By correctly metering the proper water flow, any equilibrium temperature of the thermal plate above the cold source temperature can be maintained. Very fine temperature control can be achieved by metering slightly more cold water than is required (slightly overcooling the Primary Circuit) and adding electrical energy with the use of the emersion heater. Both emersion heater output and flow of water through the trickle pump are under servo control of the control computer.

A second pump is included in the secondary hydraulic circuit in order to provide rapid changes of thermal plate temperature during the step ("PAUSE") period shown in Figure 4. The surge pump is operated full on for a period ranging from about one to seven seconds, depending upon the magnitude of the desired temperature decrease in the warm plate. A relatively large parcel of cold water is displaced into the Primary Circuit during this period, causing a rapid drop in temperature. A period of about 10 to 30 seconds is required for temperature equilibrium. The surge pump is not used again until another change in plate temperature is desired. The hydraulic circuit for the cold plate is similar to that described above except that the surge pump for the cold plate is attached to a separate TEM-powered heat exchanger (Hot Source), controlling temperature of water above the mean temperature of the experiment. Operation of the surge pump for the cold circuit raises the temperature of the cold plate, such that the temperature difference between the plates is reduced in steps as the experiment progresses.

A third heat exchanger is available on the instrument to circulate water at the mean temperature of the experiment over temperature-sensitive equipment. This control is used to provide cooling to the following areas:

8

- Water at the temperature T_m is circulated through a water jacket over the sample injection tube in order to condition the sample aerosol at T_m. This provides a convenient reference temperature, allowing the influence of the dynamic viscosity of the aerosol on the rate of flow to be taken into account. The rate of flow of the sample into the chamber must be known to an accuracy of 1%. Other important flow capillaries are also conditioned in this way.
- Conditioning the flow of the sample to T_m also serves to raise the relative humidity of the sample air, allowing the aerosol particles to grow large, and effectively reduce the aerosol particle diffusion coefficient of the sample in the sample injection tube. Aerosol particle diffusion losses are designed to be kept below about 1% in the CFD.
- Water at T_m is circulated behind the exit wall of the chamber in order to limit droplet evaporation as the aerosol cloud particles pass from the chamber into the optical particle counter. Water at T_m is also circulated through a heat exchanger to condition the protective sheath flow of air provided by the OPC to limit droplet evaporation.

The effect of evaporation of droplets in the optical particle counter seems to be somewhat unknown at this time, and is potentially quite important when the mean temperature of the cloud-forming experiment approaches the lower limits.

Therefore, if accuracies of the order 1% are attempted for the cloud-forming experiment, it would seem necessary to gain more knowledge than is presently available on the effects of droplet evaporation in the exit of the continuous flow diffusion chamber, and in the OPC.
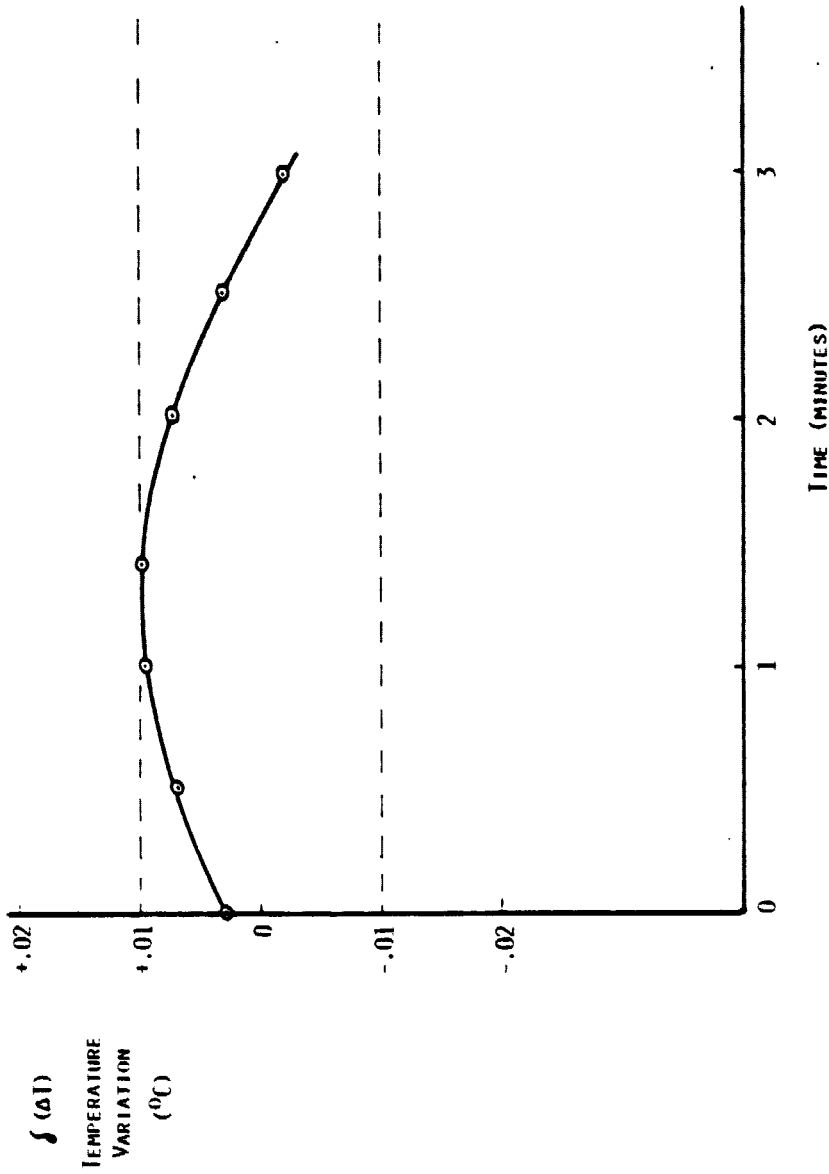
4.0   TEMPERATURE MEASUREMENT

Thermal performance of the system has proven to be quite good. Knowledge of the temperature difference between the plates and its stability are the critical determinations made in the operation of the CFD; the design goal for plate temperature uniformity and knowledge of the differential

9

temperature measurement between plates in the critical region of the chamber was ±0.01°C. Figure 6 shows the variation in the ΔT measurement for a period of three minutes. Time zero in this experiment represents the beginning of the second "LWAIT" period, as shown in Figure 4, just after a change in plate temperature has occurred. Figure 7 shows the variation in the ΔT measurement for a period of four minutes after allowing the experiment (LWAIT Period) to proceed for eight minutes. In both presentations, the resolution of the temperature measurement is 0.0024°C.
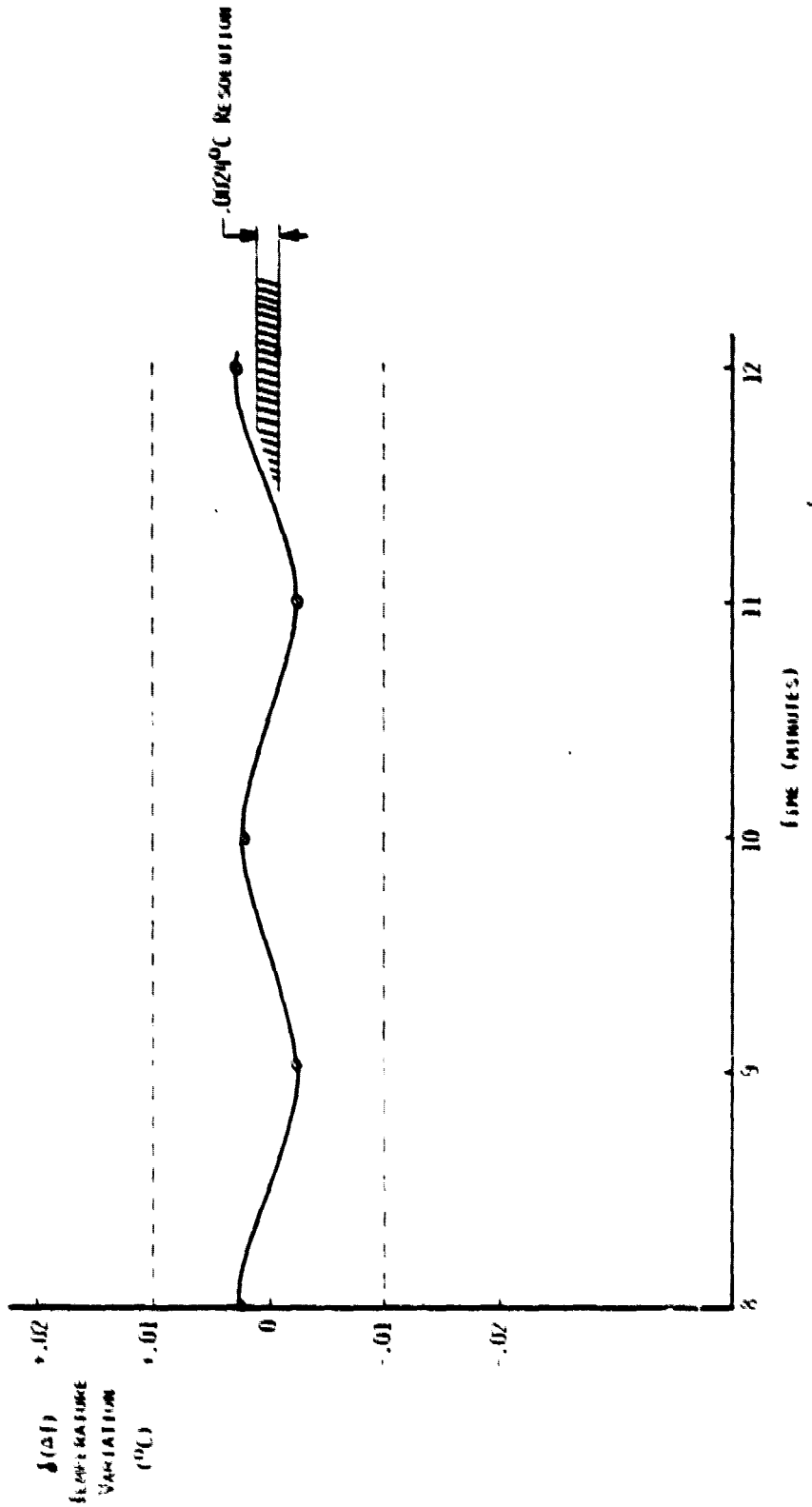
The ΔT measurement is accomplished with the use of a ten-element thermopile mounted on the back surface of each thermal plate. The thermocouple junctions are chromel-constantan and are potted in good thermal contact with an aluminum base with thermally conductive epoxy. The thermopile is assembled in the form of a yoke; the thin thermocouple leads are sandwiched between two layers of grounded copper foil tape for support and electrical shielding. The entire bundle is mounted on a thin (0.04 cm x 2.5 cm) strip of fiberglass that forms a yoke around the two thermal plates. The base of the yoke mounts on the thermopile amplifier, located at the bottom edge of the CFD chamber, reducing the lead length of the thermocouples to a minimum. The resolution of measurement is 0.0024°C.

From initial experience, it appears that the long term stability of this device is on the order of one or two counts of resolution. Zero setting of the thermopile is accomplished by immersing both junctions in distilled water ice slurry, held in a large Dewar flask. The reliability of this method of zero-setting appears quite good; long periods of time are observed with no detectable drift in temperature. Drift and absolute temperature of the bath is monitored with a quartz thermometer (HP Model 2801 A), with a resolution of 0.001°C. The range of the thermopile is calibrated with two Dewars, one with ice and the other filled with distilled water. Both baths are stirred. Temperature difference is determined by measuring the temperature of each bath sequentially with the use of a single quartz thermometer probe. The use of a single probe allows an accurately known differential measurement to be made, since any absolute accuracy errors are summed out. The thermopile has been calibrated at several points using these procedures.

$\int (\Delta T)$

TEMPERATURE VARIATION AFTER CHANGING CHAMBER SUPERSATURATION. (VARIATION OF 10 JUNCTION THERMOPILE MEASUREMENT).

TEMPERATURE VARIATION ($^{\circ}C$)

+.02

+.01

0

-.01

-.02

TIME (MINUTES)

0   1   2   3

Figure 6. Variation of the plate temperature difference measurement (ΔT) starting immediately after a change in plate temperature has occurred (the second "IWAIT" period starts at time zero).

11

Figure 7. Variation of the ΔT measurement after the experiment has run for eight minutes.

The thermopile monitors the ΔT measurement only, and is not used as an active feedback control signal. All active control measurements are accomplished with the use of glass bead thermistors either immersed in water or imbedded in heat exchanger bodies. The absolute accuracy requirements of ±0.1°C for these types of measurements were much less stringent than the ΔT measurement. When the CFD system was designed, published specifications regarding long term drift of thermistors indicated that they were inadequate for making the ΔT measurement. Current literature indicates that glass bead thermistors on the market are quite stable and perhaps are suitable for this application. Our own experience with the CFD, when comparing the thermopile measurement with that of the thermistor measurement, indicates that both of these independent components are very stable indeed; agreement was obtained between the two devices within the resolution of the thermopile (.0024°C) over the 14 day period. Therefore, it might prove that the use of high quality thermistors is suitable for making the ΔT measurement. More than one thermistor could easily be used to measure a temperature distribution across the thermal plate; this is difficult to do with a thermopile because it is large and awkward. Signal amplification is also easier to do using a thermistor. Therefore, if a thermistor can be shown to have adequate accuracy and stability, it may be superior to a thermopile in this application. Because the resolution and quality of the temperature measurement systems in the new CFD are very high, it is felt that comparison of the two types of measurements over a period of time will be helpful in determining the suitability of the glass bead thermistor for measuring the temperature difference between the plates.

The thermopile was designed to allow easy removal from the CFD for periodic calibration, but in practice, this has proven a difficult task due to sealing and accessibility problems. At present, the unit is calibrated each time the CFD is disassembled for cleaning or maintenance.

5.0   TEM-POWERED HEAT EXCHANGERS

Considerable problems were encountered with the performance of all of the TEM-powered heat exchangers in the development of the CFD. These problems are discussed below.

- The walls of the heat exchangers were quite thin, and the TEM's were clamped in arrays; that is, clamping was done across several TEM's. Clamping pressure across the array of themoelectric modules caused distortion in the thin walls of the heat exchanger. Consequently, poor thermal contact between the TEM and the heat exchanger resulted, inducing a reduction of heat exchanger performance.

- A test fixture was fabricated consisting of a massive aluminum block machined flat. An array of TEM's were individually clamped to the aluminum block and the assembly was thermally insulated with rigid polyurethane form. Heat was rejected from the hot side of the TEM's using forced air cooling over fins mounted on each TEM. The temperature of the cooling fins and the aluminum block were monitored, along with the power input to the TEM array. By determining the rate of change of temperature of the aluminum block, the cooling power of the TEM could be calculated. Finally, using the measured and calculated data, actual performance of the TEM could be compared to the published performance claimed by the manufacturer.

- It was found that the performance of the TEM's mounted in the test fixture was improved over the performance observed when the TEM's were mounted on the heat exchanger, but that the COPR was still significantly lower than published claims. It is felt that good technique was observed when mounting the TEM's to the test fixture:

    (a) Both the massive aluminum block and the indi-
        vidual hot side thermal sinks were flat and
        rigid, effectively eliminating the distortion
        problem encountered with the CFD exchangers.

    (b) When removing the TEM from the test fixture,
        the pattern of the face pads of the TEM could
        be observed in the residual thermal grease
        left on the aluminum block. The grease pattern
        was very thin and quite uniform, indicating good
        thermal contact had indeed been achieved in the
        test fixture.

(c) Nylon screws were used to sandwich the
TEM to the aluminum block and the hot side
sink. High clamping pressures were
achieved. Nylon minimized heat transfer
losses through the fasteners.

(d) Ten thermoelectrics were tested, assuring
that representative performance was obtained
in the tests.

(e) Ample thermal insulation was provided to
minimize the effect of ambient losses.

The manufacturer (Cambion) was unable to offer assistance, stating that
their specifications were conservative. Nevertheless, because of the care
observed when conducting these performance evaluations, it is felt that the
modules did not meet the manufacturer's performance claims.

The performance of our heat exchangers was brought up to the required
level by incorporating the following changes:

● Individual clamping was used on each TEM to eliminate the
distortion found in our earlier design.

● The method of dissipating waste heat via forced convection
over fins was abandoned. Water jackets were constructed
and used as the hot side surface. Waste heat water was
circulated through large aluminum radiators. The result-
ing reduction in the temperature of the hot side of the TEM
provided a major increase in cooling power available.

Figure 8 shows results of a test of the cold source heat exchanger.
Performance is now higher than that expected from the original design calcu-
lations. The cold source heat exchanger has been operated below 0°C on the
CFD.

Because of the problems experienced at DRI with the use of TEM's,
it is felt that testing and evaluation of design procedures should be
accomplished early in the design phase of a major project using TEM's.
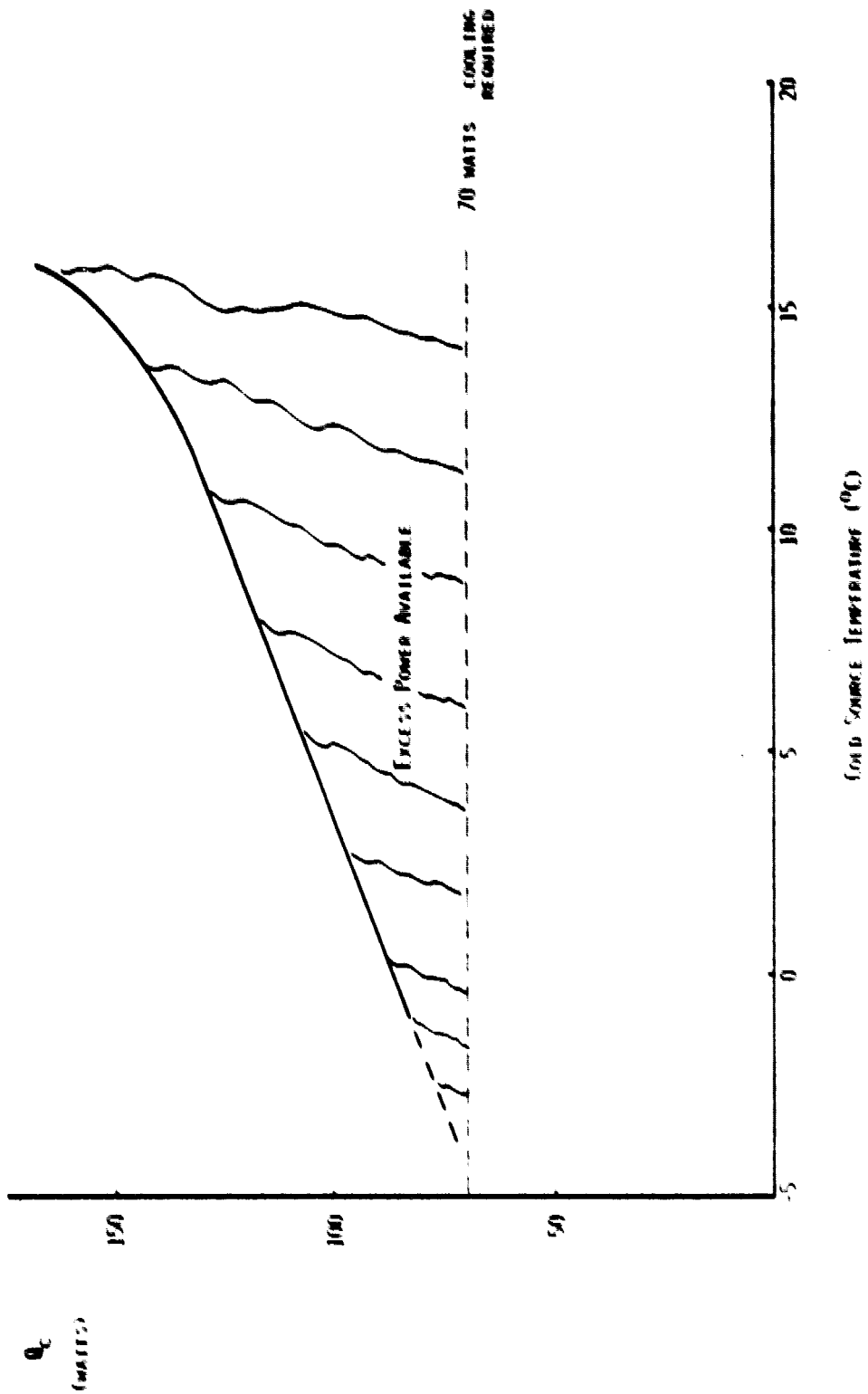
Figure 8.   Low temperature performance of the cold source heat exchanger.

6.0 WETTABLE METAL SURFACES

DRI explored the fabrication and operational characteristics of many types of metal surfaces suitable for use on the thermal plates of the CFD. Porous media of copper, stainless steel, and nickel were examined, as well as surfaces consisting of grooves machined into these materials. Machined surfaces were eventually dropped from consideration because of the following reasons:

- Originally, transverse grooves were thought to provide a means of "flushing" surface contamination away from the critical zone. However, it is felt that the shear force of the air flowing over the water surfaces dominates any effect of the water flowing in the channel grooves; therefore, any film of surface contamination would be pushed permanently to the edge of the groove.

- Several firms (Grumman Aircraft, for example) have developed the technology to machine good quality grooves. However, it was desired to develop an in-house capability regarding the fabrication of these surfaces. Development of the technology for this machining operation could have proven to be an extensive project.

- Any potential thermal conductivity advantages presented with the grooves affecting temperature measurement on the thermal plate would seem to be nullified in practice because almost all heat transfer occurs well upstream of the critical zone. In any system, this assures that very small temperature gradients are present across a thermal plate in the critical region.

Good wettability was eventually achieved by oxidizing a stainless steel material supplied by Fluid Dynamics, Inc. of Cedar Knoll, NJ. The media is a 0.032 cm thick randomly bonded mesh of micronic sized stainless steel fibers. The material chosen for the CFD plates is a special fabrication of type 304 stainless steel (Dynalloy No. 86).

The final plate configuration consisted of a 0.47 cm thick plate of OFHC copper machined with 18 water channels (.32 x .24 cm) on one side and the porous media bonded to the other. The bonding process involved

plating the surface of the copper with electroless nickel to a thickness of 0.0002 cm. The stainless steel porous media was effectively brazed to the nickel/copper interface in a hydrogen-fired oven at a temperature of 1800-2000°F.

The surface has performed satisfactorily in the CFD. Some stains are visible on the surface that apparently are associated with corrosion, but it is not known if this is a galvanic reaction of the stainless steel/copper/electroless nickel interface or if some carbide precipitation occurred in the stainless steel during the heat treatment cooling process.

Because the present design features water channels machined in a copper base with the porous media attached to the opposite surface, any damage to the porous media is serious because of the difficulty in machining copper. Futhermore, the 2000°F brazing process anneals the copper plate making it quite soft and fragile. For these reasons, our present design is not considered a good one. If a new CFD were built, the thermal plates would consist of heavier aluminum back plates with machined water channels. The porous metal wicking surface would be diffusionally bonded to a relatively thin stainless steel sheet, and would provide cover for the water channels. In this configuration, damage to the stainless steel wicking material would not require remanufacture of the channeled heat exchanger surface. This configuration was used successfully in the ACPL Saturator built for the NASA. Diffusional bonding of the porous media to the stainless steel cover sheet is done in a hydrogen-fired oven at 2000°F using a slight clamping pressure against the two clean stainless steel surfaces.

Wettability of a metal wicking surface depends upon the cleanliness of the surface. Very clean surfaces act as a sink for contamination; therefore, surfaces that are initially clean do not remain so for long if they are left unprotected in a contaminated environment. Samples left dry in room air lose their wettability after a few hours of exposure. Several methods of cleaning were used in an attempt to restore the wettability of the wicking surfaces. A three-step ultrasonic solvent process consisting of immersions in Freon 113, acetone, and hexane was tried with little success, apparently due to residual films associated with rinsing. Acid baths were attempted as well, but not too successfully because of the

18

difficulties of removing all traces of acid in the fine wire mesh
material. High temperature (∿400-500°C) oven processes can be very
effective in cleaning these surfaces. Glow discharge cleaning was
also found to be quite effective, and has the following inherent advan-
tages over the other methods:

- The method is an ambient temperature process, allowing
  heat sensitive components to be left assembled to the
  thermal plate during the cleaning process.
- No rinsing is required, eliminating any possible residual
  surface film.
- Very clean surfaces are obtained.

During recent months, DRI has developed a Glow Discharge Cleaning
apparatus, consisting of a vacuum system, a large bell jar (44 cm dia. x
74 cm length) and an RF power supply. The cleaner is versatile, in that
a variety of cleaning configurations can be set up and cleaned in this
system. The apparatus is especially useful because the entire CFD chamber
can be inserted in the bell jar, and by utilizing the thermal plates of
the CFD as RF field plates, the wicking surfaces can be cleaned in situ;
that is, the plates can be cleaned without violating the chamber air-seal.
This is a major step forward in increasing the utility of the CFD as a labo-
ratory instrument because of the reduction of assembly and testing that can
be achieved with this cleaning concept. Because the outer aluminum case
must still be removed from the current CFD, it is estimated that the total
cleaning operation will require about 6-8 hours. This is about 20 to 30%
of the time previously required for this operation. If a new CFD were to
be built, the chamber itself would be utilized as the vacuum chamber,
reducing the cleaning time to about two hours. This concept is shown in
Figure 9.

The CFD was recently disassembled so that the cleanliness of the
porous metal wicking surfaces could be examined. These surfaces had
accumulated about 2 1/2 months of exposure inside the chamber. The sur-
faces were assembled wet and maintained wet in the chamber during this
period. All air entering the chamber other than sample air was filtered
through a large activated charcoal canister. Cleanliness of the porous
metal wicking surfaces was evaluated qualitatively by visually exmaining
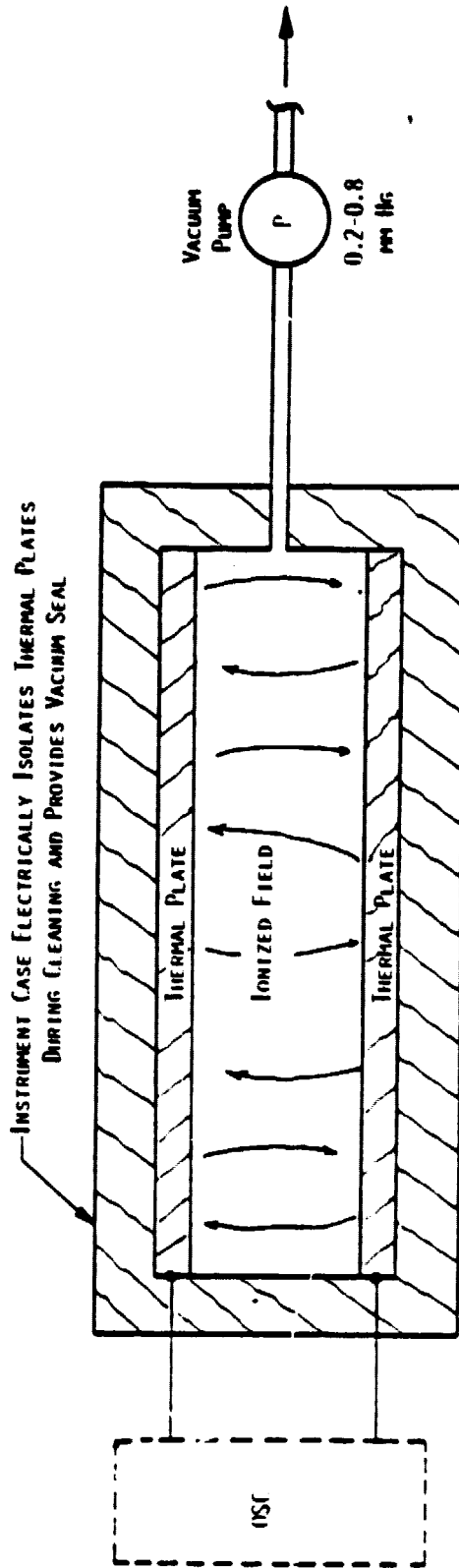the rate of wetting and the uniformity of the flow pattern of distilled

Figure 9. GLOW DISCHARGE CHAMBER CLEANING CONCEPT

Much effort can be saved and cleaner wet surfaces can be realized if assembly and handling of the wicking surfaces can be kept at a minimum. This concept utilizes the metal wicking surfaces as field plates.

Filling wicking surfaces with water immediately after cleaning reduces contamination of these clean surfaces.

water being drawn through the wicks via capillary action. These tests
indicated that the surfaces were surprisingly clean; very little degra-
dation of the wettability of the wicking surfaces had occurred since the
freshly cleaned surfaces were originally installed in the chamber. More
exposure time and experience will be obtained in future work with these
surfaces; however, these preliminary results indicate that the metal wick-
ing surfaces probably will require infrequent maintenance when the CFD
is used in the laboratory.

It is felt that charging the wicking surface with distilled water
immediately after cleaning is an effective means of reducing surface con-
taminations. Wetting apparently reduces the exposure of the clean sur-
faces to contamination.

7.0   SAMPLE INJECTION SYSTEM

The design and calibration of the sample injection system were given
a great deal of attention in order to meet performance requirements of the
program. The primary design goals were set to maximize the aerosol par-
ticle survival rate of the sample flow in the chamber, and to obtain a
sample flow rate measurement accuracy of 1%. The following steps were
taken to limit particle diffusion.

- The flow is augmented in three places by auxiliary or
  dump flows.
- The sample is controlled to the mean temperature of the
  experiment in order to increase the relative humidity of
  the sample and hence, increase particle size. The result
  is a reduction of the particle diffusion coefficient.
- Boundary layer suction is provided in the sample exit
  slit manifold in order to strip away the depleted boundary
 layer that would be associated with established laminar
  flow.

Figure 10 schematically represents our sample injection system.

The flight hardware contractor has used the DRI sample injection
design approach with two modifications. The first modification consists
of measuring the flow across the sample slit only, so that one flow

21
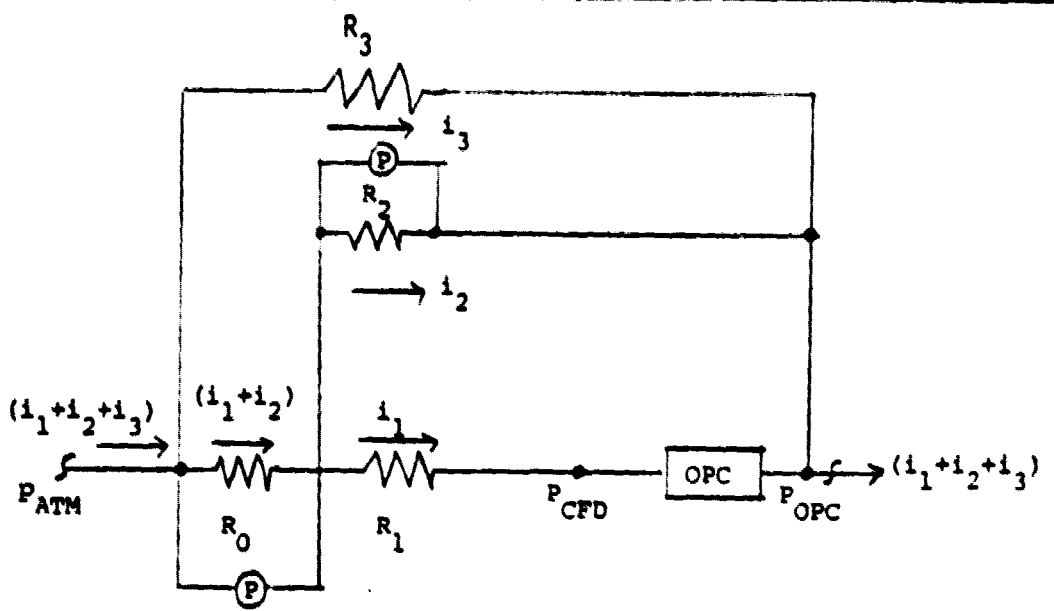
FLOW SCHEMATIC

R_0 = Capillary Resistor [(i_1+i_2) measured here]

R_1 = Resistance of 8.0 cm x .050 exit section

R_2 = Resistance of porous walled tube + adjusting capillary [i_2 measured here]

R_3 = [i_3] dump flow capillary
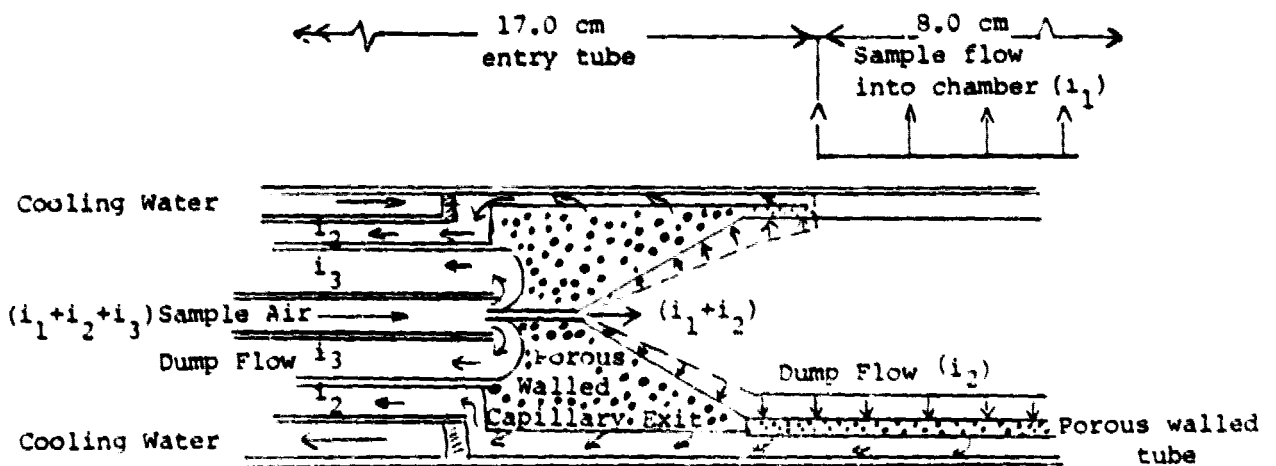
BOUNDARY LAYER CONTROL CONCEPT

Dump Flow i_3 = 10 cc/s

Dump Flow i_2 = 0.1 cc/s

Sample Flow i_1 = 0.2 cc/s   ($0.2 \leq i_1 \leq 0.8$ cc/s)

Figure 10.   Upper flow schematic shows system of auxillary dump flows used to inhibit sample diffusion. Stagnant boundary layer is removed from sample slit manifold as shown in lower tube cross-section.

22

measurement is made instead of two, as in the DRI approach. This is a
major reduction in component complexity, and furthermore, allows a more
precise measurement of sample flow to be taken, since the error associated
with the second flow measurement is reduced to zero. Two disadvantages
arise, however; the lack of ability to easily change (for instance, by
changing an external capillary) the dump flow out of the porous wall of
the sample exit-slit manifold makes the effect of this flow very diffi-
cult to evaluate experimentally. With external control of this flow, the
experimenter can observe changes in the particle survival rate while
increasing or decreasing this dump. In order for this to be a viable
method, precise measurement of the dump flow (i_2 in Figure 10) is
required. Furthermore, when using an external capillary it is easy to
tune the flow rate to any desired value simply by changing capillaries
if it is found that the original flow rate is found not to be optimum.

The second modification to the DRI design concept is to provide an
additional dump flow out the end of the sample slit manifold. This would
seem to be a design improvement as long as this flow is kept reasonably
small.

Verification of the particle survival rate in the sample injection
system is quite difficult to accomplish when accuracies of order 1% are
desired; however, this is an extremely important parameter when the per-
formance of different types of cloud-forming instruments are compared.
It would seem appropriate to experimentally verify the diffusion loss
characteristics of the sample injection system in a program of experi-
ments such as those planned for ACPL. A diagram of a diffusional loss
experiment performed with the DRI sample injection system is shown in
Figure 11. Using this apparatus, particle counts of sample passing through
the "control experiment" was sequentially compared with counts of sample
passing through the CFD sample injector. Because of problems of sample
decay during storage, a better experiment would consist of running a con-
trol configuration simultaneously with the sample injector using "tuned"
CFD's and optical particle counters. This would allow various parameters
affecting diffusional losses to be changed and the effects would immediately
and accurately be detected. Also, it should be possible to determine the

23
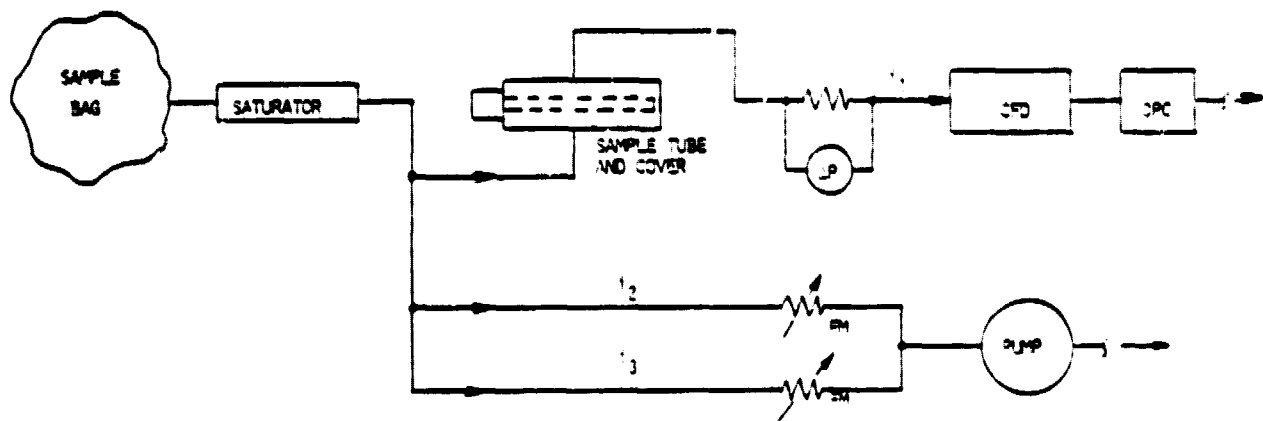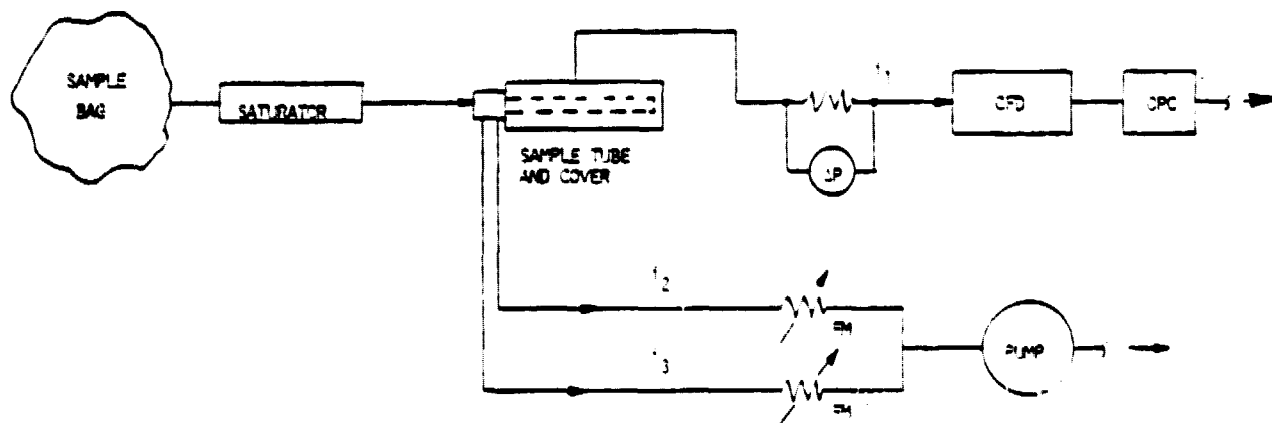
Figure 11. Schematic of diffusion loss experiment performed at DRI.
Sample loss in the Control Experiment was compared sequentially
with that in the Diffusion Loss Experiment.

absolute survival rate quite accurately using these procedures. Using the sequential experiment, DRI could not detect any loss of particles through the fully operating sample injection system; however, due to the effect of particle loss in the storage bag ($\sim$10% per hour) the estimated error of the experiment could have allowed for several percent of unobserved losses during this test.

Flow rate measurement is accomplished in the DRI CFD by measuring the pressure drop across calibrated stainless steel capillaries. Calibration of these capillaries to 1% accuracy proved a formidable task. The most critical calibrations were carried out by displacing a soap bubble in a glass burette of known volume and timing the full displacement with a stopwatch. Dry air was used in the capillary; therefore, the effects of water vapor in the air from the soap solution, on the volume measurement, had to be taken into account theoretically. The source of pressure was provided by a Texas Instrument model 156 Precision Pressure Test Set modified by the DRI. This unit utilizes a quartz pressure transducer. Ordinary sources such as bottled air controlled by two stage regulators proved unsatisfactory at the accuracy level of 1%. Effects of viscosity change with temperature on the flow calibration could easily be seen using our system.

The CFD pressure transducer and amplifier system was used to measure pressure during the calibrations in order to reduce any possible errors of conversion. Performance of the pressure measuring system was monitored using the quartz pressure transducer in order to evaluate effects of changes of temperatures and other environmental characteristics. It was found that the Setra instruments selected for this design met all of the performance claims of the manufacturer as long as adequate insulation from local ambient changes in temperature and pressure were provided. Unprotected transducers gave unreliable and erratic readings; the units seemed to be extremely sensitive to rapid rates of change of temperature, and to pressure fluctuations caused by local air currents. Wrapping the units in cottom seemed to be effective in eliminating these problems.

Position of Sample Injection

The sample tube is mounted on an eccentric mechanism which can be rotated and thus moved to various distances from the two parallel plates. The supersaturation profile is a maximum near the central plane and goes

25

to zero at both plate surfaces. This, and because gravitational forces (in horizontal 1-g operation) and phoretic forces move the particles and/or drops toward the cold plate, points to the fact that injecting the sample at the mid-plane may not always result in optimum performance.

8.0 CONTROL ELECTRONICS

Due mostly to very conservative design, few problems have arisen in the prototype control system. However, two electrical problems which have appeared caused considerable difficulty in testing and initial system operations.

Amplifier Breakdown Problem. Figure 12 shows a typical circuit by which devices consuming considerable power are controlled by computer output. The same circuit is used for all proportionally controlled DC devices, and was originally built without the fuse and zener diode shown within the dashed line square. Prior to this addition, LM324 amplifiers were damaged at irregular intervals. Although no significant transients were ever discernable on any of the lines, the amplifiers were protected by clamping the input power line. The problem has not reoccurred in over 100 hours of testing nor has the fuse opened. The problem apparently stemmed from extremely short (i.e. low energy) transients between the 28 VDC and DC commonline. The method of repair is somewhat marginal although it seems adequate for our present usage. A preferable approach may be either to isolate the 28 V source to the LM324 amplifier (perhaps with a 28 VDC/28 VDC regulated converter)* or to provide amplifiers with higher voltage ratings. More space would be required since no equivalent amplifier to the LM324 (a quad unit) is available at higher than 32 V ratings.

Thermistor Breakage. This problem is one of handling of fragile, glass rod thermistors. The small and slender thermistors were chosen for their short time constant (<0.4 sec.) when immersed in the CFD coolant fluid. Although no breakage has occurred during operation of the CFD, many have been broken while handling for calibration, etc. Possible solutions are refurbishing the CFD with stronger but slower thermistors, use of a

---

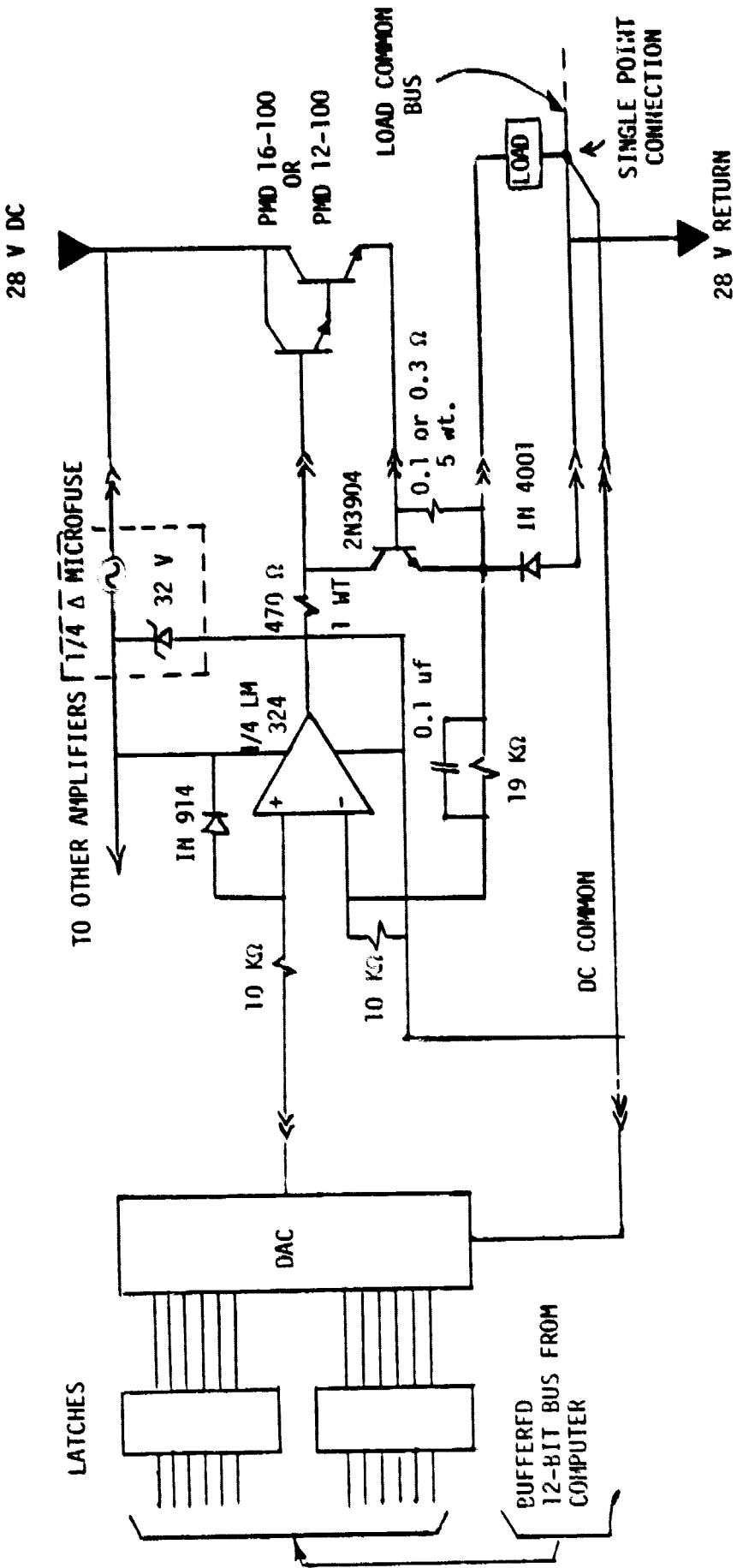*Note that the power to the amplifier should be slaved to the 28 VDC supply.

26

Figure 12. Power amplifier circuitry used for all proportionally controlled DC devices.

27

protective case or simply refined handling procedures.

The first alternatives both increase the response time. It appears that this could be tolerated with only a small effect. Refined handling techniques appear to be the simplest approach for the present CFD. At present, the many thermistors are wired to their sensing electronics through connectors with several thermistors per connector. In a new design, it would be advantageous to wire one per connector in order to facilitate repair of broken units.

The present CFD uses redundant thermistor measurements for each temperature measurement, so that in case of a failure of one unit, operation of the CFD system can continue with a minor change in programming.

9.0   REFERENCES

Hudson, J.G. and P. Squires, 1973: Evaluation of a recording continuous cloud nucleus counter. J. Appl. Meteorl., 12, 175-183.

Hudson, J.G. and P. Squires, 1976: An improved continuous flow diffusion cloud chamber. J. Appl. Meteorl., 15, No. 17.

Baier, R.E. and V.A. DePalma, 1970: Electrodeless glow discharge cleaning and activation of high-energy substrates to insure their freedom from organic contamination and their receptivity for adhesives and coatings. Calspan Report No. 187, Cornell Aeronautical Laboratory, Inc.

Schlichting, H., 1968: Boundary Layer Theory, 6th Ed, Chapter XIV, McGraw Hill Book Company.

Fuchs, N.A., 1964: The Mechanics of Aerosols, The MacMillan Company, NY, pp. 204-212.

Fitzgerald, J.W., 1975: Approximation formulas for the equilibrium size of an aerosol particle as a function of its dry size and composition and the ambient relative humidity. J. Appl. Meteorl., 14, No. 6, September, 1044-1049.

Dynatherm Corporation Engineering Staff, 1972: Heat Pipe Design Handbook, Part 1, N 74-22569, National Technical Information Service.